

Target Report for Target Cell Edna

Aidan M. Kelleher, Todd D. Averett, Joseph M. Katich
The College of William & Mary
Williamsburg, Virginia 23187 USA

Gordon Cates, Vladimir Nelyubin, William A. Tobias, Jaideep Singh
The University of Virginia
Charlottesville, Virginia 22904 USA

Ameya Kolarkar
University of Kentucky
Lexington, Kentucky 40506 USA

July 25, 2007

Abstract

Jefferson Lab experiment 02-013 benefited from a breakthrough in target polarization technology. This was the first experiment using a polarized helium-3 target to use hybrid alkali metal spin-exchange optical pumping. This change led to a higher in-beam polarization. The target cell used to collect data for two data points at the end of the E02-013, had the highest polarization of the new hybrid cells.

1 Introduction: Experiment 02-013

Knowledge of the neutron electric form factor G_E^n is essential for an understanding of nucleon structure. In simplest terms, the Fourier transform (in the Breit or “brick wall” frame) of G_E^n is the charge density of the neutron. Recent measurements on the proton show that the ratio (G_E^p/G_M^p) declines sharply as Q^2 increases. Therefore the electric and magnetic form factors (of the proton) behave differently above $Q^2 \approx 1(\text{GeV}/c)^2$. At this time, there is scant data on the behavior of G_E^n as we move beyond this Q^2 value.

The form factors are key ingredients of tomographic images developed through the framework of Generalized Parton Distributions (GPDs). GPDs are universal functions that supersede both the well known parton distribution functions (observed *via* deeply inelastic scattering) and form factors (observed *via* elastic electron scattering.) GPDs allow calculation of a wide class of hard exclusive

reactions[1]. Form factor results are used to constrain the GPD models[2]. Information about G_E^n is important to constrain the electric GPD E, which presently has a large uncertainty at momentum transfers where quark degrees of freedom become essential[3].

Jefferson Lab experiment 02-013 used a double polarized asymmetry to measure the form factor G_E^n . It made use of the polarized electron beam and a modified version of the Hall A polarized ^3He target.

1.1 Introduction to Target

In order to measure a double polarized asymmetry, either a polarized target or polarimeter must be used. While there are no free neutron targets of sufficient luminosity, polarized ^3He has been used with great success as a substitute. At sufficient energy transfers, the neutron is considered almost free. The orientation of the proton spins (anti-aligned due to the Pauli principle) means that approximately 90% of the spin of the ^3He is in the neutron. These combine to produce an effective polarized neutron target.

In Hall A, the procedure used is spin-change optical pumping (SEOP). The principle of SEOP was developed in the last 25 years[4]: circularly polarized laser light excites the ground state electrons of an alkali metal in a magnetic field. This quickly polarizes all of the atoms of the alkali metal. Polarization is then transferred from the alkali metal atoms to the noble gas nuclei by means of a hyperfine-like interaction between the valence electron of the alkali metal and the noble gas nucleus.

1.2 Introduction to Edna

For this experiment, there were two types of cells produced – one with a 2.5” diameter pumping chamber and another with a 3.5” diameter pumping chamber. To easily distinguish between the two styles, a naming convention was used. The smaller size pumping chamber was given male names, and the other style was given female names. The names would be given in alphabetical order. Edna was the fifth cell with a large pumping chamber.

Edna was made by Mike Souza at Princeton University. It was filled and characterized by Al Tobias and Vladimir Nelyubin at the University of Virginia. It was mounted in place on March 28, 2006 and was used until the end of the experiment on May 10, 2006.

2 Magnet Box

The distinguishing feature of previous ^3He experiments was a set of crossed Helmholtz coils. For this experiment, the coils are gone. In their place is a large iron box. This box serves as a shield for the fringe fields coming from BigBite. The box has 4 sets of 2 coils (8 total). They are arranged in such a way to produce a uniform field in across the width of the box.

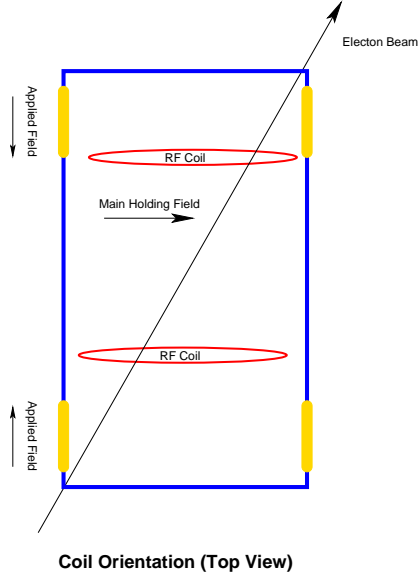


Figure 1: **Magnet Box.** The magnetic field was generated by energizing coils that generated a field in a piece of iron.

2.1 Magnetic Inductance

A major concern in using coils wrapped around an iron box to generate the magnetic field used to polarize the target was the possibility of a non-linearity in the ramp used to produce the spin flip required to measure the polarization. It was assumed that the non-linearity would be due to hysteresis in the iron. Careful measurements were made to investigate this possibility. The tests showed a linear “up sweep”, and a “down sweep” with minor variations from linearity. In short, no hysteresis effects were observed.

When the linearity was checked, it was assumed that the dominant contribution to a nonlinearity would be from the hysteresis. The field was stepped, a measurement was made, and the field was stepped again. This would be sufficient to detect hysteresis effects, but not time dependent effects. In the course of running the experiment, a time dependent effect was discovered.

In order to perform an AFP NMR measurement (see section 3.1), the field must be sweep from a low to high field value and back again. In other words, during the AFP NMR measurement, the field is time dependent. A pronounced lag can be noticed between the voltage sent to the coils and the field produced. Investigations of this effect indicate that is due to the inductance of the coils. This inductance is small for open core coils, but becomes large when iron is introduced into the coils, as is the case for E02-013.

This is an interesting effect that will be dealt with in greater detail in a forth-

coming comprehensive paper on the target polarization. However, it should be sufficient to note that this effect can have no effect on the target polarization numbers presented in this report. The effect is a line shaping effect, but it will be the same for both the NMR measurements used to extract a polarization constant and the NMR measurements used to monitor the polarization. Analysis of NMR signals used demonstrate that his effect is consistent. This line shaping effect will have an overall effect on the error due to the fit for each NMR measurement. However, this uncertainty is small compared to the uncertainty due to the calibration constant (roughly 0.6% vs. roughly 4.5%).

3 Polarimetry

In previous experiments using a polarized ^3He target, two methods of measuring the polarization were used. The first is the straightforward method of adiabatic fast passage nuclear magnetic resonance (AFP NMR or just NMR), where the spins of the ^3He are flipped, and the resulting signal is directly related to the polarization. The second is electron paramagnetic resonance (EPR), where the alkali atoms are used as incredibly sensitive magnetometers. They are so sensitive that the polarization is measured through the shift in the magnetic field around the atoms due to ^3He polarization.

These were independent measurements in the past, with the NMR signal calibrated to the known thermal polarization of water. For this experiment, EPR, with it's precise absolute polarization measurement, was used to calibrate NMR. The straightforward NMR, which is measured in the scattering chamber, was used as a day to day check on the polarization.

3.1 NMR

Through this document, the term NMR refers to a specific type of nuclear magnetic resonance. The specific type is nuclear magnetic resonance seen through adiabatic fast passage (AFP). AFP is a method of reversing the spins of polarized ^3He gas. In simple terms, this spin reversal is performed by changing the magnetic field while applying a crossed high frequency (91kHz) magnetic field. If this change is performed slowly enough, it will be an adiabatic change and the spins will follow. However, the change must be fast enough that the spins do not have time to relax. This relatively fast spin reversal produces an EMF in nearby pickup coils. This EMF is what is commonly referred to as our NMR signal.

3.2 EPR

Simply put, the method of electron paramagnetic resonance uses light from the target cells alkali metals as a precise magnetometer. This magnetometer is used to measure the small change in the magnitude of magnetic field due to polarized ^3He that is either aligned or anti-aligned with the main holding field.

There are two shifts in the Zeeman response of Rb and K in the presence of polarized ^3He . There is a shift due to the same spin exchange mechanism that produces the polarization in the gas [5]. There is also a shift due to the presence of a classical magnetic field of the polarized ^3He . These shifts can be isolated by changing the direction of the magnetic field.

The shift due to the magnetic field due to the magnetic field produced by the polarized ^3He is proportional to the ^3He magnetization (and therefore the density and polarization of the ^3He [6]:)

$$\Delta\nu_b = \frac{d\nu_{EPR}(F, M)}{dB} CM_{He} = \frac{d\nu_{EPR}(F, M)}{dB} C n_{He} \mu_{He} P_{He} \quad (1)$$

where \vec{K} is the ^3He nuclear spin and C is a dimensionless quantity that depends on the shape of the sample. For a spherical sample, combining the shifts due to collision and classical magnetic field, we obtain:

$$\Delta\nu_{EPR} = \frac{8\pi}{3} \frac{d\nu_{EPR}(F, M)}{dB} \kappa_0 \mu_{He} P_{He} \quad (2)$$

where κ_0 is a constant that depends on temperature that has been measured experimentally[7].

3.2.1 How Do We Measure It?

This change in frequency depends on many things, but the small shift that is due to the magnetization of ^3He is the only shift that depends on the direction of the ^3He spins. Therefore, we can isolate the shift if we can change the direction of the spins while keeping everything constant. We do this by means of frequency sweep AFP (applying an oscillating field that is in resonance with the ^3He nuclei's precession in an applied magnetic field – this is very similar to how NMR is performed).

We measure the frequency before and after the “flip”. This isolates everything else and leaves us with (twice) the frequency shift due to the ^3He polarization.

$$\nu \uparrow - \nu \downarrow = \nu_{all} - \nu_{all} + \nu_{^3He\uparrow} - \nu_{^3He\downarrow} \quad (3)$$

But,

$$\nu \uparrow = -\nu \downarrow \text{ and } \nu_{^3He\uparrow} = -\nu_{^3He\downarrow}$$

Fig.2 is an drawing of how this measurement is performed.

3.3 Locking the Frequency

The EPR transition is excited by broadcasting an RF frequency signal through a coil. We scan across a frequency to find the transition, and then lock to that transition.

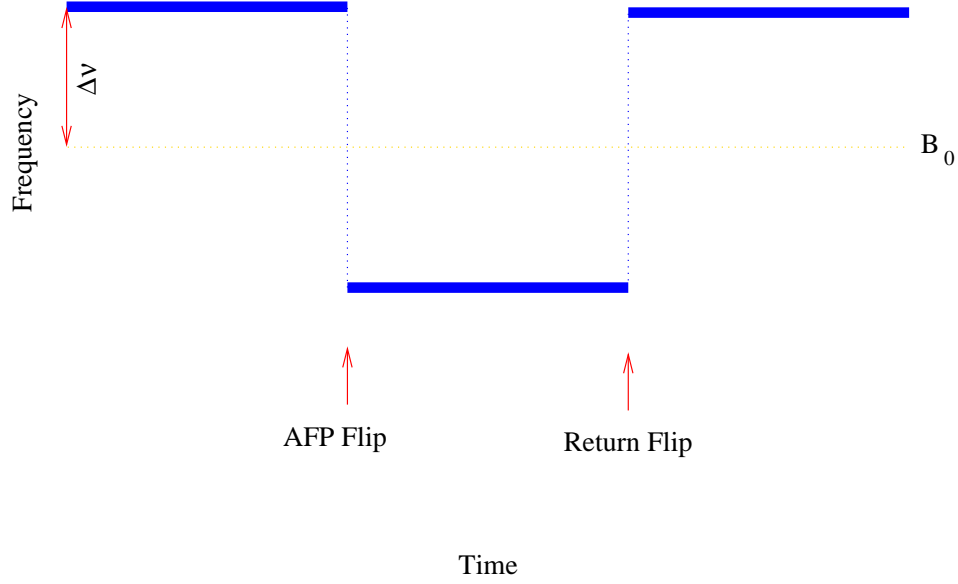


Figure 2: **EPR Measurement.** Example of EPR measurement with features of interest to target expert noted.

Exciting the EPR transition depolarizes the alkali metal (Rb, for simplicity). Once the alkali metal depolarizes, it begins to re-polarize. This produces a fluorescence. We can track the amount of fluorescence as a function of RF frequency. Because our RF frequency is FM modulated, we see the derivative of the EPR transition line-shape. We lock to the zero of the derivative (so, a maxima or minima, but we know it's the local maximum), using a feedback loop.

Once the frequency is locked, the AFP sweep can begin. At the moment of resonance, all the ^3He spins flip. The feedback system can track the EPR frequency during this flip and the system is locked to the new EPR frequency. In this state, the ^3He spins are anti-aligned with the alkali metals are polarization direction, so a return flip is required to prevent depolarization.

3.4 Magnitude and Direction of B_0

This measurement of the polarization also provides “free” information about the magnitude of the magnetic field and orientation of the ^3He spins with respect to the magnetic field.

As seen in Fig. 2, the magnitude of B_0 can be extracted from the frequency about which the EPR transitions occur. This has proved to be an incredibly precise measurement of the magnetic field in the location of the EPR measurement. For E02-013, this effectively means we measured the magnetic field about once a day.

State	Flip?	Spins
Hat	Flipped	Aligned
Well	Not Flipped	Anti-Aligned

Table 1: **The States of the Spins.** The alignment of the spins with the magnetic field can be determined from the shape of the EPR signal

Direction of the ^3He spins, cannot be determined directly from the EPR data. However, once the magnetic holding field direction is known, it is a simple matter to determine if the spins are aligned or anti-aligned relative to the holding field. One needs to combine this information with some other measurement to determine the direction of the ^3He spins with respect to an external coordinate system.

In the case of a frequency shift above the holding field shift (“well” state, pictured in Fig. 2), the effective field seen by the alkali metal is the holding field plus the classical field of the polarized gas. For the “hat state” (not pictured), the field subtracts.

Recall that the magnetic moment for ^3He is negative, and the neutron spins are aligned with the ^3He spins, and the neutron spins are aligned with the ^3He spins. This means that if the field is adding, then the spins (of both the neutron and ^3He) are pointed opposite the magnetic field. Table 1 should clear this up.

3.4.1 Hybrid EPR

When only one alkali metal is used in the cell, EPR is a straightforward proposition. For the hybrid cells, there is a mixture of two alkali metals. The EPR response of either metal can be monitored by the fluorescence of the metal being pumped.

In Rb-K hybrid cells, the spin exchange between Rb and K are so efficient that at any point in time the polarizations of the two metals are identical. It is this property that allows the K to polarize the ^3He without being pumped directly. However, it is also this property that allows EPR to be performed on either metal. Exciting the EPR transition in K depolarized the K. The depolarized K depolarizes the Rb, the process of re-polarizing the Rb causes the Rb to fluoresce.

The depolarization of interest comes from exciting the EPR transition in the alkali metal in the cell. In the case of a hybrid cell, either alkali metal can be depolarized. In either case, we use the D_2 line of the metal that is optically pumped. It is possible to use the amount of D_2 light of one metal (e.g. Rb) to monitor the depolarization of another (e.g. K) because the spin exchange cross section for Rb and K is extremely large [8]. In this way, the Rb polarization serves as a real time monitor of the K polarization.

3.5 Target Density

The ^3He cell has 8 resistive temperature devices (RTDs) attached to various locations. These RTDs are constantly read out via the Hall A EPICS system. Since they are placed on the outside of the cell, localized internal heating (*e.g.* from laser energy absorption in the pumping chamber) is not registered by the RTDs, due to the temperature gradient across the thick (approximately 4mm) glass wall. To correct for this a series of temperature tests are performed on the cell to gauge the true temperature of the gas within.

These tests are a series of NMR measurements. First, the NMR signal is measured with the lasers on. Then lasers are turned off, and the cell is allowed to reach equilibrium. Then, another NMR measurement is performed. Once the depolarization effects due to performing the NMR measurements are taken into account, the relative difference in signal height gives an indication of change in density. The change in density, combined with the measurement of the target chamber temperature, gives the true pumping chamber internal gas temperature.

3.5.1 Theory

The NMR signal can be expressed as the product of a number of factors:

$$S_{NMR} = P \cdot n_{^3\text{He}} \cdot \Phi \cdot \mu_{^3\text{He}} \cdot C_{electric} \quad (4)$$

Where $C_{electric}$ are factors due to the electronics used, $\mu_{^3\text{He}}$ is the ^3He magnetic moment, Φ is the flux through the coils, $n_{^3\text{He}}$ is the number of ^3He atoms that generate that flux and P is the polarization of those atoms. When performing the temperature tests, we will be looking at the ratio of signals, this reduces the equation to an expression that depends solely on the polarization and density.

$$\frac{S_{on}}{S_{off}} = \frac{P_i n_{on}}{P_{i+1} n_{off}}$$

$P_i > P_{i+1}$, since there is a depolarization of the ^3He each time that an NMR measurement is made (referred to as AFP loss). Once the correction due to AFP loss is made, the equation simplifies even further.

$$\frac{S_{on}}{S_{off}} = \frac{n_{on}}{n_{off}} \quad (5)$$

Since the volumes are the same, the NMR signal effectively functions as a pressure gauge. The number of atoms in the target chamber (n) can be determined from the known volumes, and the ratio of the temperatures.

$$n_t = \frac{n_o}{1 + \frac{V_p}{V_o} \left(\frac{T_t}{T_p} - 1 \right)} \quad (6)$$

Equation 6 follows from the ideal gas law. Although the density of the cell (n_o) at uniform temperature is known, it is not required, since the ratio of the target chamber with the lasers on (n_{on}) to the density with the laser off (n_{off}) is required. The approximation $T_{t\ on} \approx T_{t\ off} = T_t$ is supported by the data. There are only slight fluctuations, which are consistent with fluctuations if the target pumping chamber temperature is stable.

$$\frac{S_{on}}{S_{off}} = \frac{n_{on}}{n_{off}} = \frac{1 + \frac{V_p}{V_o} \left(\frac{T_t}{T_{p\ off}} - 1 \right)}{1 + \frac{V_p}{V_o} \left(\frac{T_t}{T_{p\ on}} - 1 \right)} \quad (7)$$

3.5.2 Experimental Method

There are two series of tests that must be performed for an accurate laser on/off temperature test. The first is the hot AFP loss test, the second is the laser on/off temperature tests.

3.5.3 AFP Loss Tests

When an NMR measurement is performed on the E02-013 $^3\vec{H}e$ target, there is a small loss in the polarization. This loss is particular to the type of NMR measurement performed. Since we use adiabatic fast passage NMR, this loss is commonly referred to as ‘‘AFP loss’’. There are many factors that contribute to the AFP loss. There are gradients in the magnetic holding field, impurities in the glass of for the cell, *etc.* While it would be possible to calculate these contributions to the AFP loss, it is much more straightforward to merely measure this loss. Observations of this loss indicate that the loss changes with temperature. Due to the variety of contributions to the loss, both temperature dependent and independent, it is again much more straightforward to measure the loss than to attempt to calculate it.

The measurement of this loss is very direct. With the cell in an equilibrium state (close to maximum polarization and little recent interaction with the electron beam), the lasers are turned off. The temperature of the cell is allowed to stabilize. Once the temperature is stabilized, a number of NMR measurements (typically 5-10) are performed. The result is a clearly visible loss per measurement, as seen in Figure 3.

It would be tempting to fit such a plot to a line and look at the slope. The problem with this tactic is that the loss should be added to each point. To go from point zero to two the loss should be added twice. The proper fit for this is a decaying exponential. However, with only five measurements, the preferred method is to look at the difference between each measurement and compare to the first measurement. Results are listed in Table 2.

3.5.4 Lasers On/Off Tests

The next step is to collect the data with the lasers on and off. First, with the cell at equilibrium, a single NMR measurement is made. Then, the lasers are turned

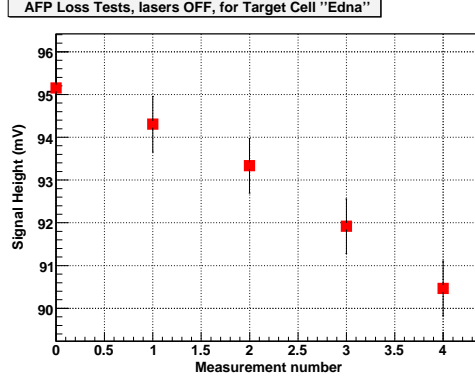


Figure 3: **AFP Loss Test.** Multiple NMR measurements are performed and the average loss per measurement is calculated

off and the cell is allowed to cool. This cooling takes about 10 minutes. The temperature is monitored via a stripchart display. When the cell temperature flattens out, the next NMR measurement is made. Once this measurement is made, the lasers are turned back on and the cycle repeats. For Edna the cycle was repeated four times

In the case of Edna, the temperature stabilized approximately 5°C below the previous set-point. The time between measurements was approximately 10 minutes. Figure 4 shows the clear separation between the lasers on and lasers off. It is also clear that the “slope” is similar to that of the AFP loss test. Once the AFP loss corrections have been made, the differences are even clearer, as in Figure 5

3.5.5 Results

Table 2 lists the results for the AFP Loss test. The average of the losses are 1.24% for the up sweep and 1.27% for the down sweep. The value of 1.26% loss per measurement was used to correct the signals for the lasers on/off test. A similar dataset exists for the AFP loss at the operational temperature with the laser on. It should not be a surprise that the AFP loss is less when the lasers are on. The average of the losses for lasers on are 1.07% for the up sweep and 1.12% for the down sweep. The average of these losses is 1.10%.

Table 3 lists the temperature for each measurement in the lasers on/off test. The control RTD and RTD 7 are the measurements for the temperature in the oven (measured on the cell). RTDs 1, 2, 3, and 5 are measurements on the target along the target chamber. All measurements are in degrees Celsius. A striking feature of this table is the lack of variation between measurements for the RTDs on the target chamber. This is the justification for the approximation made in Section 3.5.1; $T_{t\ on} \approx T_{t\ off} = T_t$.

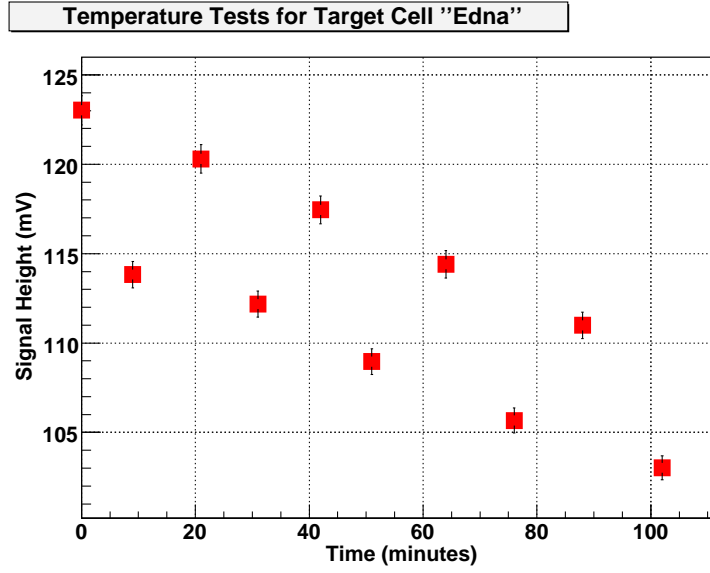


Figure 4: **Uncorrected Lasers On and Off.** There is a clear separation between measurements made with the lasers on and off.

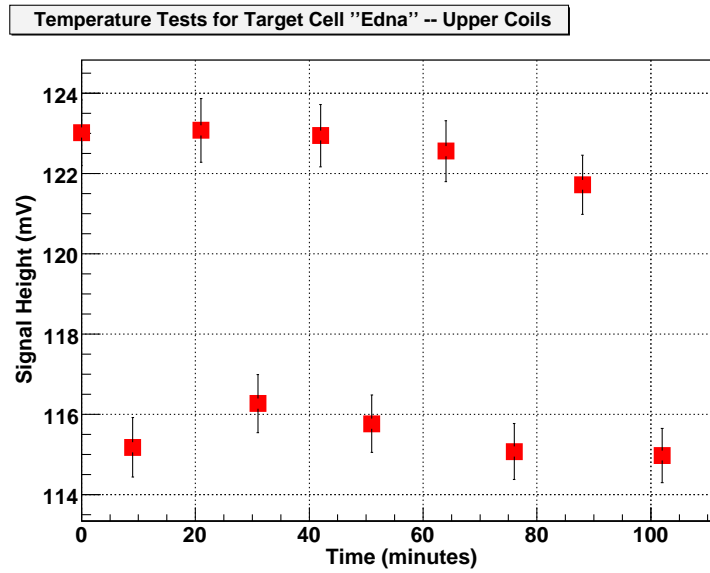


Figure 5: **AFP Loss Corrected Lasers On and Off.** With the AFP corrects added, the separation between measurements with the lasers on and off is very clear; the measurements can also be seen to group together.

Table 4 contains the corrected values from the laser on off tests. Each value on the table (except for the first ones) are corrected based on whether or not the lasers were on during the previous measurement.

The parameters used for the calculation of the temperature with the lasers on are listed in Table 5. Given these values, we can go back to Equation 7. Note: V_o is the total volume of the cell.

$$\frac{S_{on}}{S_{off}} = \frac{1 + \frac{V_p}{V_o} \left(\frac{T_t}{T_{p\ off}} - 1 \right)}{1 + \frac{V_p}{V_o} \left(\frac{T_t}{T_{p\ on}} - 1 \right)}$$

From Table 5, the ratio following useful ratios are formed:

$$\frac{S_{on}}{S_{off}} = 1.0625 \quad (8)$$

$$\frac{V_p}{V_o} = 0.7730 \quad (9)$$

$$\frac{T_t}{T_{p\ off}} = 0.6086 \quad (10)$$

What remains is to find $\frac{T_t}{T_{p\ on}}$.

$$1.0625 = \frac{1 + 0.773(0.6086 - 1)}{1 + 0.773 \left(\frac{T_t}{T_{p\ on}} - 1 \right)}$$

$$\frac{T_t}{T_{p\ on}} = 0.5556$$

$$\frac{T_t}{0.5556} = T_{p\ on}$$

$$T_t = 308.77K$$

$$T_{p\ on} = 555.74K$$

$$T_{p\ on} = 282.59^\circ C$$

$$\Delta T = 39.63^\circ C$$

3.6 Polarization Gradient

Polarimetry for $^3\vec{H}e$ target in Hall A is typically performed with a combination of EPR (see Sec. 3.2) and NMR (see 3.1). These two independent measurements are used as a cross check against each other. In previous experiments, NMR measurements are calibrated against an NMR signal generated by thermally polarized water. For the experiment E02-013, no such water calibration was performed. Therefore, the EPR measurement was not a cross check against the NMR calibration, but instead the only calibration for the NMR measurement.

The main difficulty with using this method for NMR calibration lies in the relative position of the two measurements. EPR is performed in the upper of the

Measurement	Up (mV)	Down (mV)	Loss Up	Loss Down
1	94.945	95.361	—	—
2	94.167	94.448	0.82%	0.96%
3	93.199	93.470	1.03%	1.04%
4	91.784	92.057	1.52%	1.51%
5	90.328	90.601	1.59%	1.58%

Table 2: **AFP Loss Results.** The results of the AFP loss tests performed with the lasers off, and the cell at its working temperature of approximately 250°C.

Measurement	control rtd	rtd 7	rtd 1	rtd 2	rtd 3	rtd 5
On 1	240.9	245.6	39.2	38.0	32.3	33.8
Off 1	235.8	233.3	39.4	37.8	33.9	32.0
On 2	241.0	245.2	39.1	39.7	33.7	32.5
Off 2	235.9	233.4	39.1	39.7	33.7	32.1
On 3	240.7	244.7	39.2	37.7	33.8	32.5
Off 3	235.4	232.7	39.1	37.6	33.5	32.0
On 4	240.8	244.7	38.9	37.7	33.4	32.3
Off 4	234.6	232.2	38.9	37.4	33.4	31.8
On 5	241.0	245.0	39.0	37.5	33.4	32.2
Off 4	236.1	232.9	38.6	37.5	33.3	31.9

Table 3: **Lasers On/Off Temperatures.** The temperatures listed (in degrees Celsius) were taken before each measurement.

Measurement	Up (mV)	Down (mV)	Average (mV)
On 1	122.8	123.3	123.0
Off 1	115.2	115.2	115.2
On 2	122.8	123.4	123.1
Off 2	116.1	116.5	116.3
On 3	122.6	123.3	122.9
Off 3	115.5	116.1	115.8
On 4	122.2	122.9	122.6
Off 4	114.6	115.5	115.1
On 5	121.3	122.2	121.7
Off 5	114.6	115.3	115.0
Average On	122.3	123.0	122.7
Average Off	115.2	115.7	115.5

Table 4: **Corrected Laser On/Off Values.** NMR values from the laser on/off values that have been corrected for AFP losses

Parameter	Value
T_t	35.62°C
$T_{p\ off}$	234.23°C
$T_{p\ on}$	242.96°C
V_o	377.73 mL
V_p	292 mL
S_{on}	122.67 mV
S_{off}	115.45 mV

Table 5: **Calculation Parameters.** Parameters used in the calculation of the true temperature in the pumping chamber when the lasers are on.

two chambers. This is the chamber where the ^3He gas is polarized (“pumping chamber”). NMR measurements are performed in the lower of the two chambers. This chamber is where the electron beam interacts with the polarized gas (“target chamber”). See Fig. 6.

After the ^3He is polarized in the pumping chamber, it must diffuse through the thin transfer tube before reaching the target chamber. Once the ^3He atoms leave the pumping chamber, they are no longer affected by the polarized Rb and K. They therefore begin the spin-relaxation process. This results in a lower polarization. It must be the case the polarization in the target chamber is lower than the polarization in the pumping chamber. The expression that best explains our situation is:

$$P_t^\infty = P_p^\infty \frac{1}{1 + \frac{\Gamma_t}{G_t}} \quad (11)$$

Where G_t is the diffusion rate, Γ_t is the depolarization rate and P_t^∞ and P_p^∞ are the equilibrium polarizations in the target chamber and the pumping chamber, respectively. Equation 11 will be derived in section 3.6.1.

The factors of G_t can be separated into 3 groups. There are geometrical factors relating to the volume of the pumping chamber and the length and area of the transfer tube. There are factors that are intrinsic chemical properties of ^3He gas. And there are factors that are related to the relative density and temperature of the gas in the two chambers. The first two groups of terms are well known. The last group – the density and temperature of the gas – can fluctuate throughout the experiment and cannot be directly measured during the experiment.

Γ_t not only depends on the these temperature and density parameters; it also depends on the depolarization due to the electron beam.

3.6.1 Theory

As ^3He gas flows from one chamber to the other, it is no longer in contact with the polarized alkali metal, and starts to depolarize. We can think of a

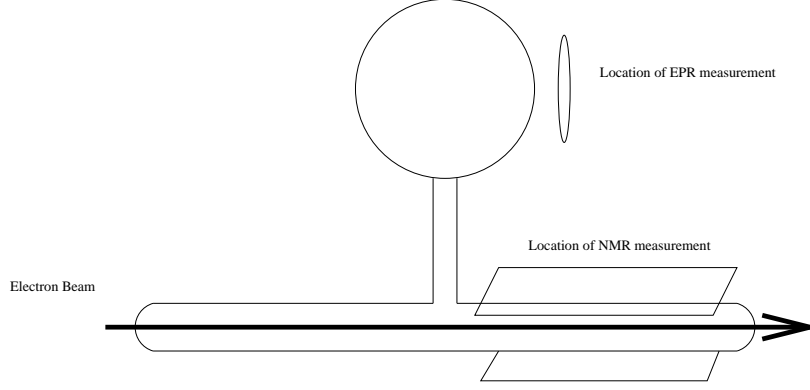


Figure 6: **Relative Position of Measurements.** The NMR measurements are made in the same location as the electron beam interaction; however, the EPR measurement used to calibrate is in another location.

polarization current that flows from one chamber to the other.

$$J(z) = \frac{1}{2}n(z)D(z)\frac{dP}{dz} \quad (12)$$

Where $n(z)$ is the density of helium and $D(z)$ is the diffusion coefficient. Both are functions of position along the transfer tube due to the thermal gradient. After conserving the current and integrating along the transfer tube, we get

$$J = \frac{1}{2}D_t \frac{n_t}{L} K (P_p - P_t) \quad (13)$$

K is a constant that depends on the ratio of temperatures in the target and pumping chambers.

$$K = (2 - m) \frac{1 - \frac{T_p}{T_t}}{1 - \left(\frac{T_p}{T_t}\right)^{2-m}} \quad (14)$$

D_t is the diffusion coefficient at the target chamber.

$$D_t = D(T_o) \frac{n_o}{n_t} \left(\frac{T_t}{T_o}\right)^{m-1} \quad (15)$$

The rate of change in polarization due solely to diffusion (for each chamber) is therefore

$$\frac{dP_p}{dt} = -\frac{2JA_{tr}}{n_p V_p} \quad (16)$$

$$\frac{dP_t}{dt} = \frac{2JA_{tr}}{n_t V_t} \quad (17)$$

Finally, we are left with the following for the change in polarization due to diffusion.

$$\frac{dP_p}{dt} = -\frac{A_{tr}}{V_p L} \frac{n_t}{n_p} D_t K (P_p - P_t) \quad (18)$$

$$\frac{dP_t}{dt} = \frac{A_{tr}}{V_t L} D_t K (P_p - P_t) \quad (19)$$

This almost completely describes the polarization in the target chamber, since the polarized gas can only come from the upper chamber. The gas in the upper chamber, however, is continually polarized. The change in polarization in the upper chamber is

$$\frac{dP_p}{dt} = -\frac{A_{tr}}{V_p L} \frac{n_t}{n_p} D_t K (P_p - P_t) + \gamma_{SE}^{Rb} P_{Rb} + \gamma_{SE}^K P_K - (\gamma_{SE}^{Rb} + \gamma_{SE}^K + \Gamma_p) P_p \quad (20)$$

The target chamber polarization only needs a correction due to the depolarization effects in the target chamber.

$$\frac{dP_t}{dt} = \frac{A_{tr}}{V_t L} D_t K (P_p - P_t) - \Gamma_t P_t \quad (21)$$

For ease of notation,

$$G_t = \frac{A_{tr}}{V_p L} D_t K$$

Consider P_t^∞ and P_p^∞ , the equilibrium cases, then set equation 21 equal to zero. The equilibrium polarization of the target chamber in terms of the pumping chamber polarization is therefore:

$$P_t^\infty = \frac{P_p^\infty}{1 + \frac{\Gamma_t}{G_t}} \quad (22)$$

In principle this equation has everything that we need to determine the relationship between the two chambers. In reality, we need to take this a step or two further. When the beam is on (or has recently been on, as is the case for most of our EPR calibrations), we need to determine the effect of the beam on the polarization.

$$\Gamma_t^{beamON} = \Gamma_t^{beamOFF} + \Gamma_{beam} \quad (23)$$

We do not have a direct measurement of $\Gamma_t^{beamOFF}$ for our in-hall setup. However, it can be approximated at a very high level from the data taken at UVa.

We have NMR signals at times where the beam was on and the beam was off. This will allow us to extract the polarization. Another way to write the

polarization in the chambers makes this clear:

$$P_{p,t}^{BeamON} = \frac{P_{K,Rb} < \gamma_{SE} >}{< \gamma_{SE} > + < \Gamma > + f_t \Gamma_{beam}} \quad (24)$$

$$P_{p,t}^{BeamOFF} = \frac{P_{K,Rb} < \gamma_{SE} >}{< \gamma_{SE} > + < \Gamma >} \quad (25)$$

$$= \frac{P_{K,Rb} < \gamma_{SE} >}{\gamma_{spinup}} \quad (26)$$

Where f_t is the fraction of particles in the target chamber, Γ_{beam} and γ_{spinup} is the inverse of the time constant measured for the cell; $< \gamma_{SE} >$ is the volume averaged spin-exchange rate.

Since we are measuring in the same chamber without moving the cell at all, we can take a ratio of the signals, and let the factors of flux and calibration constant cancel

$$\frac{S^{beamON}}{S^{beamOFF}} = \frac{P_t^{beamON}}{P_t^{beamOFF}} = \frac{\gamma_{spinup} + f_t \Gamma_{beam}}{\gamma_{spinup}} \quad (27)$$

$$= 1 + \frac{f_t \Gamma_{beam}}{\gamma_{spinup}} \quad (28)$$

From measurements at the University of Virginia, we have measurements of γ_{spinup} , and f_t .

$$1/\gamma_{spinup} = 6.174 \pm 0.058h$$

$$f_t = 0.325$$

3.6.2 Results

Results have been determined from the use of the temperature tests and the EPR calibrations taken with beam on and beam off. From the temperature tests we can determine the true temperature in the pumping chamber cell, and include that number in our diffusion model. Recall from Eqs. 14 and 15 that the diffusion parameters are temperature dependent. They are therefore corrected for each calibration. The average size of the correction is 5.7% with a spread of 2.5%. The depolarization lifetime due to the beam during Edna's running was:

$$1/\Gamma_{beam} = 50.8hr \pm 29.6hr$$

Due to the large uncertainty, the EPR calibrations use for the final numbers have come from the measurements with the beam off.

3.7 Calibration for E02-013

For previous experiments the relevant calibration constant between NMR and EPR can be expressed in terms of a the expression [9]:

Source	Relative Error
κ_0	4.11%
EPR Measurement	1.32%
Flux and Density	1.00%
NMR Fit	$\approx 0.6\%$
Other density	0.25%
Overall	4.47%

Table 6: **Error Budget.** The sources and relative sizes of the uncertainty for the target cell Edna.

$$c_{\text{EPR}} = \frac{S_{\text{NMR}}}{P_{\text{EPR}}(n_{\text{pc}}\Phi_{\text{pc}} + n_{\text{tc}}\Phi_{\text{tc}} + n_{\text{tt}}\Phi_{\text{tt}})C_{\nabla}C_{\tau}} \quad (29)$$

The expression is most useful to be used in comparing the calibration constant derived from water to the calibration constant derived from EPR. For this experiment we used only EPR calibrations. Therefore the uncertainty due to the corrections C_{∇} and C_{τ} is effectively zero. Likewise, we are not sensitive to the uncertainty in flux. We are only concerned with the uncertainty of the flux, in so far as it relates to the product of flux and density. That is to say, we are concerned with the uncertainty in density, and the flux tells us how to weight the uncertainty. But, this weighting factor has it's own uncertainty. Overall, the net error associate with this product is 1.00%.

We are left with the error in the ratio of S_{NMR} to P_{EPR} . Through a careful consideration of every calibration measurement with the cell in an equilibrium state, we have this number to the level of 1.32% uncertainty. Errors due to other density effects register at the sub 0.25% level.

Combining uncertainty from most sources, we have an error in our calibration constant of 1.67%. The uncertainty due to the temperature dependence of κ_0 from Eqn.2 is 4.107% at our temperatures. Additional error due to the uncertainty of the fit of roughly 0.6% is added to each data point. Overall, the average uncertainty (σ_P/P) was 4.47%, with a spread of roughly 0.01%. Clearly, the uncertainty due to κ_0 is dominant. The collected uncertainties are listed in Table 6.

3.8 Polarization for “Edna”

Edna achieved the highest in-beam polarization of any cell used in an electron scattering experiment at Jefferson Lab. At times, the cell polarization was above 50%. In addition, this cell was used continuously for over 48 days. A chart of the polarization is included as Fig.7

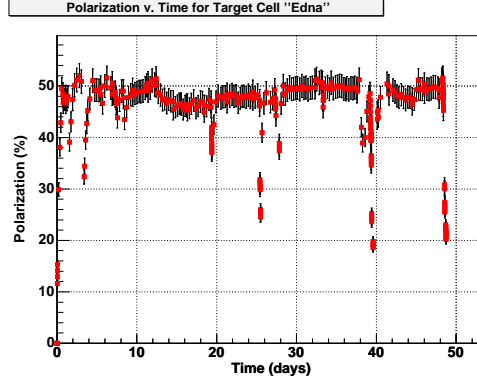


Figure 7: **Edna Polarization Measurements.** The polarization numbers for the target cell Edna, the time axis is in days from the installation of the cell. The error bars include a 4% uncertainty due to the uncertainty on κ_0 .

4 Cell Thicknesses

In order to aid in the interpretation of physics data, cell wall thicknesses for both Edna and the reference cell are included as Tables 7 & 8

References

- [1] K. Goeke, M. Polyakov, and M. Vanderhaghen, *Prog. Part. Nucl. Phys* **47**, 401–515 (2001).
- [2] M. Diehl, *Eur. Phys.J.C* **25**, 223–232 (2002).
- [3] M. Diehl, T. Feldmann, R. Jakob, and P. Kroll, *Eur. Phys. J. C* **39**, 1–39 (2005).
- [4] T. G. Walker, and W. Happer, *Rev. Mod. Phys.* **69**, 629–642 (1997).
- [5] M. V. Romalis, and G. D. Cates, *Phys. Rev. A* **58**, 3004–3011 (1998).
- [6] M. V. Romalis, *Laser Polarized ^3He Target Used for a Precision Measurement of the Neutron Spin Structure*, Ph.D. thesis, Princeton University (1997).
- [7] E. Babcock, I. A. Nelson, S. Kadlecsek, and T. G. Walker, *Phys. Rev. A* **71**, 013414 (2005).
- [8] W. Happer, *Rev. Mod. Phys.* **44**, 169–249 (1972).
- [9] K. Kramer, *A Search for Higher Twist Effects in the Neutron Spin Structure Function $g_2^n(x, Q^2)$* , Ph.D. thesis, The College of William and Mary (2003).

Right/Left	From	Distance(cm)	Thickness (mm)
n/a	Upstream	0	0.1263
Left	Upstream	3.6	1.64
		11	1.60
		20	1.60
		27.3	1.62
		3.0	1.59
	Average		1.610
Right	Upstream	3.8	1.55
	Downstream	27.0	1.64
		19.5	1.65
		12.3	1.64
		3.9	1.59
	Average		1.610
n/a	Downstream	0	0.1378

Table 7: **Cell Wall Thicknesses – Edna.** This cell was used for the third and fourth data points $Q^2 = 2.6\text{GeV}^2$ and $Q^2 = 3.5\text{GeV}^2$

Right/Left	From	Distance(cm)	Thickness (mm)
n/a	Upstream	0	0.1278
Left	Upstream	2.8	0.708
		11.5	0.815
		18.7	0.852
		13.2	0.859
		3.5	0.944
	Average		0.8356
Right	Upstream	4.1	1.10
		12.2	0.84
		19.4	0.812
	Downstream	10.9	0.784
		4.3	0.849
	Average		0.8766
n/a	Downstream	0	0.122

Table 8: **Reference Cell Wall Thicknesses.** This cell was used to measure background from glass and nitrogen in the cell.

- [10] G. Cates, K. McCormick, B. Reitz, and B. Wojtsekhowski, Jefferson lab experiment 02-013 (2002).